

Design and Performance of Compensated Reluctance Synchronous Machine Drive with Extended Constant Power Speed Range

Maarten J. Kamper, *Senior member, IEEE*, and Wikus T. Villet
Department of Electrical and Electronic Engineering
Stellenbosch University
Stellenbosch, South Africa
kamper@sun.ac.za

Abstract—Reluctance synchronous machine drives are known to be efficient, however are also known to have a poor constant power speed range. Interior permanent magnets are normally used in the reluctance synchronous machine to improve the constant power speed range. In this paper an alternative reluctance synchronous machine drive that extends the constant power speed range without using permanent magnets is proposed and investigated. In the proposed drive the DC-link current is used through a compensating or assisting field winding on the rotor. The analysis and design aspects of such a reluctance machine are presented in the paper. The results show, amongst others, that the proposed drive can generate constant power up to 3.5 per unit speed and improve the power factor of the machine in certain cases by more than 20%.

I. INTRODUCTION

Energy efficiency is becoming of major importance in variable speed drives. This is due to the increasing percentage of generated electric power that is converted to mechanical power via electric machine drives. The use of permanent magnets (PMs) in drive motors is starting to play an important role to improve the efficiency of the drive. However, the volatility in availability and cost of PMs, and the loosing of robustness due to possible magnet demagnetization, again puts the focus on so-called non-PM machine drives. In this regard the induction machine, switched reluctance machine and reluctance synchronous machine (RSM) drives are important.

The RSM drive has the advantages of using a standard drive inverter and control, manufacturing its rotor is less energy-intensive than manufacturing the cast aluminum cage rotor and can be designed to have reasonably low torque ripple. The most outstanding feature of the RSM drive is its higher operating efficiency compared to that of the induction machine drive [1] [2]. It is thus interesting that industry shows new interest in RSM drives due to efficiency and the RSM drive is a non-PM drive.

The RSM drive, however, has two major drawbacks.

The research work presented in this paper is financially sponsored by the National Research Foundation (NRF) in South Africa.

First, it needs accurate sensorless position estimation for best performance and for robustness. Secondly, the RSM drive has a very limited constant power speed range (CPSR). A third disadvantage of the RSM drive is the higher kVA rating of the inverter due to the lower RSM power factor; the higher kVA rating of the inverter has a cost and efficiency implication. Of these three disadvantages the second disadvantage of the poor field weakening performance is probably the worst. The RSM is, due to its saliency rotor, quite suitable for sensorless position estimation by using high frequency injection and fundamental saliency estimation methods. Studies, however, show that in certain low-load and high-load torque regions of the machines the position estimation can fail.

The question is if it is possible to solve, at least to a certain extent, the above-mentioned three disadvantages of the RSM drive, i.e. without using additional permanent magnets or power converter? In this paper an alternative RSM drive is proposed and investigated, in which the DC-link current of the drive is used to feed a compensating or assisting field winding wound on the RSM rotor. The investigation and evaluation of the feasibility of the proposed drive is done on a four-pole RSM at 1.4 kW power level.

II. SALIENT SYNCHRONOUS MACHINES FOR DRIVES

The use of an additional field winding on the rotor of the RSM as proposed in this paper, puts this machine in the category of wound rotor DC-excited synchronous machines. A separate DC-DC voltage-fed current-controlled power electronic converter is normally used to power the d-axis field rotor winding and to actively control the rotor field flux [3] [4].

Fig. 1 gives a spectrum of salient (reluctance) synchronous machine options for drives. Saliency in Fig. 1 is indicated by the internal flux barrier in the rotor. In the diagrams the dq reference frame is shown fixed to the rotor. The machine options vary between the RSM of Fig. 1(a) on the one hand and the interior permanent magnet (IPM) machine of

Fig. 1(e) on the other hand. Between these machine options there is first the compensated RSM (C-RSM) of Fig. 1(b), where a compensating winding is put on the negative q-axis of the rotor to compensate for (or oppose) the q-axis stator flux. The machine in Fig. 1 (c) is defined as an assisted RSM (A-RSM) where the field winding is put on the d-axis of the rotor to assist the stator's d-axis flux; this machine is the normal salient wound rotor synchronous machine. A d-axis field winding is also used on the rotor of the machine of Fig. 1(d), but a permanent magnet is added that is directed in the negative q-axis direction to compensate for the stator q-axis flux. This machine can be seen as a hybrid biaxial excited synchronous machine where both magnets and field winding are used as proposed by [5].

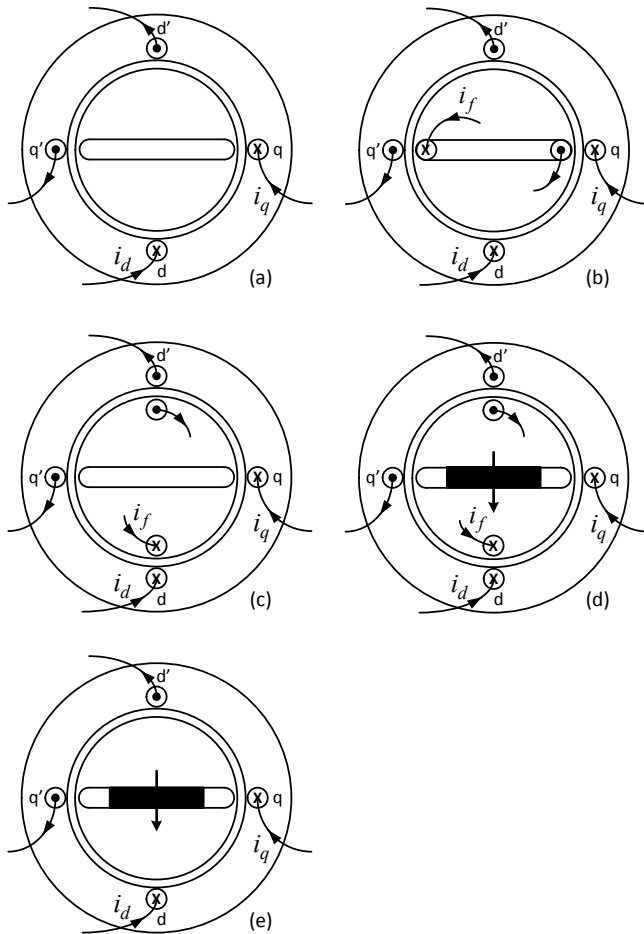


Figure 1. Salient (reluctance) synchronous machines: (a) RSM, (b) C-RSM, (c) A-RSM, (d) hybrid biaxial and (e) IPM.

III. PRINCIPLE OF PROPOSED DRIVE

In this paper the focus is on the first three machines of Fig. 1, i.e. the RSM, the C-RSM and the A-RSM. The RSM considered in this study implies a synchronous machine with a good saliency rotor design using internal flux barriers [6]. It is shown that this RSM in a variable speed drive performs very well in the sub-base speed region of the drive. In the above-base speed region with flux weakening and the inver-

ter voltage at its maximum, the control of the dq currents becomes difficult specifically due to the relative high q-axis flux linkage. Hence, the RSM rapidly loses torque with increase in speed above base speed [7]. The RSM drive, thus, does not have a performance problem in the sub-base speed region, but only in the above-base speed region.

To make a wide CPSR possible for the RSM drive, permanent magnets are normally used in IPM rotor machines to decrease the stator q-axis flux (Fig. 1(e)). These machines are sometimes referred to as PM-assisted RSMs. It is proposed in this paper that use be made of a compensating winding on the rotor q-axis to reduce the stator q-axis flux linkage (Fig. 1(b)). This compensation, however, is only necessary in the high speed region of the drive, as mentioned earlier. The proposed compensating q-axis rotor winding, thus, only needs to be active in the high speed region. This matches quite well with the DC-link current of the inverter. At rated torque the DC-link current builds up as speed builds up in the sub-base speed region, and only reaches rated current at base speed. At rated power the DC-link current stays at rated current in the high speed region. The proposal, thus, is to use the DC-link current as the feed-current for the compensating winding. This has the important advantage that an additional power electronic converter is not necessary.

Although the control is different and more complex, the DC-link current can also be used as feed-current in the case of the A-RSM of Fig. 1(c). In this case the stator q-axis flux is not reduced, but the d-axis stator current. This improves, amongst other things, the power factor of the machine. This option is also partly investigated in this paper.

A concept diagram of the proposed compensated or assisted RSM drive is shown in Fig. 2. The following must be noted in this regard:

(i) With faulty brushes and/or faulty rotor winding the switch S shown in the DC-link in Fig. 1 can be closed and the RSM drive can still operate at full capacity up to base speed.

(ii) The inductance of the compensating or assisting winding adds to the DC-link filter inductance or can be used as the filter inductance of the drive, hence saving cost. The rotor winding connected in the DC-link, thus, is not detrimental to the drive, except for the resistance voltage drop which causes the DC-link input voltage to the inverter to drop.

(iii) Using the DC-link current for the compensating or assisting rotor winding, implies that the number of turns of this winding is very much fixed. It is in this case, thus, not possible to have a high number of field turns and a low field current.

(iv) Using a rotating high frequency voltage injection method for sensorless position estimation, a high frequency induced voltage in the rotor winding may be measured at the terminals of the DC-link. It is reckoned that this voltage signal, which is available at the drive controller, can give additional information about the position of the rotor. Also the induced voltage in the rotor winding due to machine slotting may be used to estimate rotor speed.

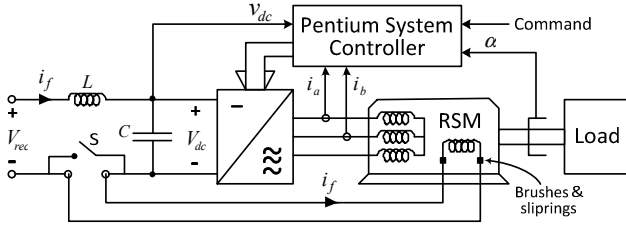


Figure 2. Proposed DC-link rotor current RSM drive system.

The disadvantages of the drive are also clear, namely it needs a set of brushes and slip rings, it needs a five-core power cable from the inverter to the machine and it uses a more expensive rotor due to the wound compensating or assisting winding. The use of brushes and slip rings, however, in certain applications is not uncommon [3] [4] [5].

IV. MODELLING OF COMPENSATED AND ASSISTED RSM

The dq steady-state equivalent circuits used in the analysis and the space phasor diagram of the C-RSM are shown in Fig. 3; the circuits and phasor diagram for the A-RSM are self-evident. The developed torque of the RSM in the dq reference frame fixed to the rotor is given by

$$\tau = \frac{3}{4} p (\lambda_d i_q - \lambda_q i_d). \quad (1)$$

In (1) λ_d and λ_q are the resultant d-axis and q-axis stator flux linkages respectively, and i_d and i_q are the d-axis and q-axis stator currents. The resultant stator flux linkages and the resultant rotor field winding flux linkage, λ_f , are expressed for the q-axis (compensated) wound rotor as

$$\begin{aligned} \lambda_d &= \lambda_{ds} = L_d i_d \\ \lambda_q &= \lambda_{qs} - \lambda_{qf} = L_q i_q - L_{qf} i_f \\ \lambda_f &= \lambda_{ff} - \lambda_{fq} = L_f i_f - L_{fq} i_q, \end{aligned} \quad (2)$$

and for the d-axis (assisted) wound rotor as

$$\begin{aligned} \lambda_d &= \lambda_{ds} + \lambda_{df} = L_d i_d + L_{df} i_f \\ \lambda_q &= \lambda_{qs} = L_q i_q \\ \lambda_f &= \lambda_{ff} + \lambda_{fd} = L_f i_f + L_{fd} i_d. \end{aligned} \quad (3)$$

The current i_f in (2) and (3) is the rotor field current, which is also the DC-link current as shown in Fig. 2. For a given stator current $\mathbf{I}_s = i_d + j i_q$ and given field current i_f in the FE analysis, the resultant dq stator flux linkages are calculated for a skewed rotor by using the Park transformation matrix $[\mathbf{K}_p]$ as

$$[\lambda_{dq}] = [\mathbf{K}_p] \frac{1}{k} \sum_{n=1}^k \lambda_{abc}(\alpha_n). \quad (4)$$

In (4) $\lambda_{abc}(\alpha_n)$ denotes the total phase flux linkages of the unskewed machine at rotor position α_n and is calculated by means of 2D static finite element (FE) analysis. The effect of skew is accounted for by using a set of unskewed machines of which the rotors are relatively displaced by an angle that is a fraction of the total skew. In (4) we use $k = 5$ unskewed

machines, which implies that only five FE static solutions are required to determine the dq flux linkages. If the ripple in the flux linkages versus rotor position is too high, then the average must be determined over a slot pitch or a 60° electrical pitch by position-stepping the rotor in the FE analysis.

With the dq flux linkages known, the speed voltages $e_d = -\lambda_q \omega_r$ and $e_q = \lambda_d \omega_r$ of the equivalent circuits of Fig. 3 are determined, where ω_r is the electrical speed of the rotor reference frame. The core losses, P_c , are calculated from the loss-frequency curves of the laminations and the FE-determined teeth and yoke flux densities. With P_c known the core loss resistance r_c in Fig. 3 is calculated as

$$r_c = \frac{3E_s^2}{P_c} \quad \text{with} \quad E_s = \sqrt{\frac{e_d^2 + e_q^2}{2}}. \quad (5)$$

The dq end-winding flux linkages are represented in Fig. 3 by the terms $\lambda_{de} = L_e i_{d1}$ and $\lambda_{qe} = L_e i_{q1}$. The end-winding inductance L_e is calculated separately by means of an analytical formula. The stator resistance, r_s , is also calculated analytically by using a practical filling factor and at an assumed temperature of 75°C . With the parameters and dq currents of the equivalent circuits known, the circuits can be solved and the *rms* supply phase current and phase voltage can be calculated as

$$I_{s1} = \sqrt{\frac{i_{d1}^2 + i_{q1}^2}{2}}; \quad V_s = \sqrt{\frac{v_d^2 + v_q^2}{2}}. \quad (6)$$

From this the supply power and copper losses of the stator and rotor windings are determined as

$$\begin{aligned} P_s &= 3V_s I_{s1} \cos \theta \\ P_{cus} &= 3I_{s1}^2 r_s \\ P_{cuf} &= i_f^2 r_f, \end{aligned} \quad (7)$$

where θ is the power factor angle as defined in Fig. 3. Note from (7) that P_s is the supply power from the inverter and P_{cuf} is an additional field loss component. With an approximate function value for the wind and friction losses known, and assuming the efficiency of the inverter for this study as unity, the efficiency of the compensated or assisted RSM drive can be determined.

Assuming a lossless inverter and space vector modulation at a unity modulation index, the supply voltage V_s of (6) must be according to

$$V_s \leq 0.407V_{dc} + \Delta V, \quad (8)$$

where ΔV is an additional constant *rms* voltage allowing for proper current control, and where V_{dc} is given by

$$V_{dc} = V_{rec} - i_f r_f. \quad (9)$$

Note that (9) takes into account an important volt drop in the DC-link of the drive caused by the compensating or assisting rotor winding as shown in Fig. 2.

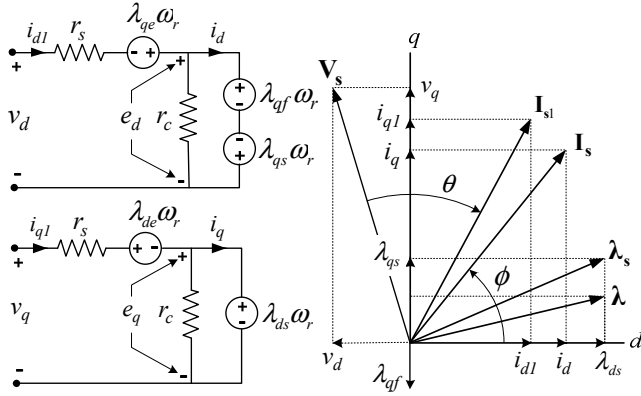


Figure 3. DQ circuits and space phasor diagram of the C-RSM.

V. RSM ROTOR WINDING DESIGN

In the design of the wound rotor winding the efficiency of the C-RSM and A-RSM drives must be at least the same or higher than the conventional RSM drive. The compensated and assisted rotor windings, thus, must be designed to have an optimum number of turns using the maximum allowed slot area available in the rotor to reduce P_{cuf} of (7).

A. Compensated rotor winding

To determine the turns for the compensating rotor winding two conditions must be valid, namely (i) there must be balance between the stator q-axis and the rotor q-axis MMFs and (ii) there must be power balance between the machine's input power and the DC-link power. For the MMF balance a simple approach is followed, namely to equal the ampere-turns per pole of the stator and rotor fields. This is given for the compensated (q-axis) rotor winding as

$$2\sqrt{2} q z_s \frac{I_s}{a_s} \sin(\phi) = \frac{i_f}{a_f} z_f \text{ (compensated)}. \quad (10)$$

In (10), a_s is the number of parallel stator circuits, q is the number of stator slots per pole per phase, z_s is the number of turns (conductors) per stator slot, ϕ is the current angle as shown in Fig. 3, z_f is the total number of rotor slot conductors per pole and a_f is the number of parallel rotor circuits. From (7) and (9) it follows that, for power balance,

$$i_f V_{dc} = 3V_s I_s \cos \theta. \quad (11)$$

The rated field (DC-link) current can be determined approximately by

$$i_{f(\text{rated})} \approx \frac{P_{m(\text{rated})}}{\eta_{RSM} \eta_{inv} V_{rec}}, \quad (12)$$

where $P_{m(\text{rated})}$ is the rated mechanical shaft power of the uncompensated RSM, and η_{RSM} and η_{inv} , the rated machine and inverter efficiencies respectively of the uncompensated RSM drive. With i_f known, an initial value for z_f can be determined from (10) by using the rated current and current angle of the RSM. With i_f and z_f and also ϕ as inputs to the FE model, the stator current that satisfies the power balance of (11) can be

determined, as explained in Section VI. This new stator current can be used again in (10) to calculate a new value for z_f . This calculation process typically converges within three iterations.

The amount of compensation depends very much on the chosen value for ϕ in (10) and in the FE analysis. If effective compensation needs to be at base speed, then typically $\phi = 50^\circ$ can be assumed; if however compensation needs to be at maximum field weakening i.e. at maximum speed, then typically $\phi = 80^\circ$ can be used. In this way typical values for z_f can be determined. In the final analysis z_f must be optimized to give the best performance for the C-RSM drive.

It is necessary to check if the value for z_f is within limits with regard to the maximum allowed field current density, $J_{f(\text{max})}$. This can be determined as

$$z_f \leq \frac{J_{f(\text{max})} A_f k_f a_f}{i_{f(\text{rated})}}, \quad (13)$$

where A_f is the total rotor winding slot area per pole, k_f is a filling factor and a_f is the number of parallel circuits of the rotor field winding.

B. Assisted rotor winding

To determine z_f for the assisted rotor winding is not that easy as it depends very much on (i) how effectively the type of rotor winding generates the field and (ii) to what extent the rotor field must assist the stator d-axis field. One method to determine z_f for the assisted winding is to first determine the rated d-axis flux linkage of the RSM, $\lambda_{d(\text{rated})}$. Then, at zero d-axis stator current ($\phi = 90^\circ$) and by using the field current of (12), z_f is increased in the FE analysis until the required percentage of rated d-axis flux linkage is obtained, subject obviously to the constraint of (13). Again, in the final analysis z_f must be optimized to give the best overall performance over the entire speed range of the A-RSM drive.

VI. PERFORMANCE SIMULATION

To simulate the steady-state performance of the RSM drives, the best performance of the drive at a number of speeds is determined by a developed simulation method that uses the above-described FE analysis, subject to the constraint of (8) and the power balance of (11). The best performance is defined as maximizing the efficiency and the shaft power of the machine, however with the shaft power not higher than rated power.

To determine the performance of the machine at a certain speed the field current, current angle and frequency are given as inputs, and the stator current that satisfies power balance is then determined. This is done as follows. With the field current known the DC input power of (11) is known. By means of FE analysis two stator currents, $I_{s(i)}$ and $I_{s(iii)}$, are determined that bracket the DC input power such that $P_{s(i)} < i_f V_{dc} < P_{s(iii)}$; note that P_s is calculated according to (7). A third power, $P_{s(ii)}$, is determined according to a third current $I_{s(ii)} = (I_{s(i)} + I_{s(iii)})/2$. The three data points of power versus

current are next used to do a curve fitting using a second-degree interpolating polynomial of the Newton form, i.e.

$$P_s(I_s) = c_1 + c_2(I_s - I_{s(i)}) + c_3(I_s - I_{s(i)})(I_s - I_{s(iii)}), \quad (14)$$

where c_1 , c_2 and c_3 are constants as expressed in (15) in the Appendix. From (14) with $P_s(I_s) = i_f V_{dc}$, the current I_s that satisfies power balance can be solved. From this the supply voltage and the performance of the drive can be determined. If (8) is not satisfied, the calculation is discarded and a next set of determined input data is used. This method uses four sets of static FE solutions to solve for the current.

Another way of simulating the performance is to obtain flux linkage data from FE analysis for all possible combinations of stator current, current angle and field current, and then post process the data to determine best performance.

VII. ANALYTICAL PERFORMANCE RESULTS

The analysis is done for a small 1.4 kW RSM. The cross section FE-model of this 24-slot machine is shown in Fig. 4. In the case of the RSM the rotor current is set equal to zero in the FE model. In the case of the C-RSM, the rotor winding current is set in the FE model to act on the q-axis, while in the case of the A-RSM, it is set to act on the d-axis. The specifications and rated performance data at 50 Hz of the RSM, C-RSM and A-RSM are given in Table I.

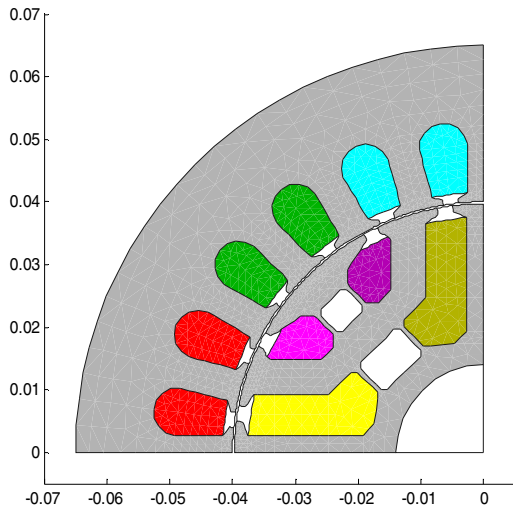


Figure 4. Cross section FE model of RSM with rotor winding.

TABLE I. SPECIFICATION AND PERFORMANCE DATA OF 1.4 KW 50 HZ CONVENTIONAL AND ROTOR-WINDING RSMs.

	V_s (V)	I_s (A)	$\cos \theta$	η (%)	Φ (°)	z_s	z_f	I_f (A)
RSM	400	3.53	0.694	82.7	57	66	-	-
C-RSM	382	3.08	0.804	82.6	53	66	310	2.83
C-RSM	377	3.02	0.826	80.9	53	66	400	2.88
A-RSM	372	2.95	0.851	83.5	75	66	310	2.8

a. d_o = stator outer diameter; d_i = stator inner diameter; g = air-gap length; ℓ = stack length; N_{ph} = number of turns in series per phase of the stator.

A. Compensated RSM

Two C-RSMs are investigated, the one with $z_f = 310$ and the other with $z_f = 400$, as also given Table I. The analytical results of the conventional and the compensated RSM drives versus speed are shown in Figs. 5 – 11. Figures 5 and 6 show that an improved torque at a lower stator current is obtained for the C-RSMs; the stator current is shown to be more-or-less 20 % less, which implies that the inverter will operate at a higher efficiency.

The shaft power and field current (or DC-link current) versus speed of the drives are shown in Figs. 7 and 8. Figure 7 shows that the conventional RSM drive has a CPSR of only 1.5 pu, while those for the two C-RSMs drives are 2.25 pu and 3.5 pu respectively. As expected, the change in field current versus speed basically follows the power trend line, as shown in Fig. 8

The power factor and efficiency performance versus speed of the drives are shown in Figs. 9 and 10. The power factor is shown to be substantially improved by the C-RSMs at speeds above base speed. In Fig. 10 it is shown that the efficiency of the C-RSM with $z_f = 310$ is the same as that of the conventional RSM up to 1.0 pu speed, but is much better at higher speeds. The efficiency of the C-RSM with $z_f = 400$ at base speed, however, is shown to be lower (1.8 %) than the conventional RSM. At this speed, thus, the machine losses exceed the allowed total power loss, which is a problem from a cooling point of view.

Finally, Fig. 11 shows the dq flux linkages versus speed of the C-RSM with $z_f = 400$. It shows how the q-axis flux is effectively compensated for and kept at a minimum throughout the speed range. The d-axis flux is shown to be reduced inversely with speed to obtain almost perfect flux weakening operation.

B. Assisted RSM

The shaft power, power factor and efficiency performance of the A-RSM with $z_f = 310$ in comparison with the C-RSM with $z_f = 310$ are shown in Figs. 12 – 14. This shows that this drive has the advantage in terms of power factor and efficiency. The only disadvantage is a reduced output power at high speeds, which is expected due to the uncompensated q-axis flux.

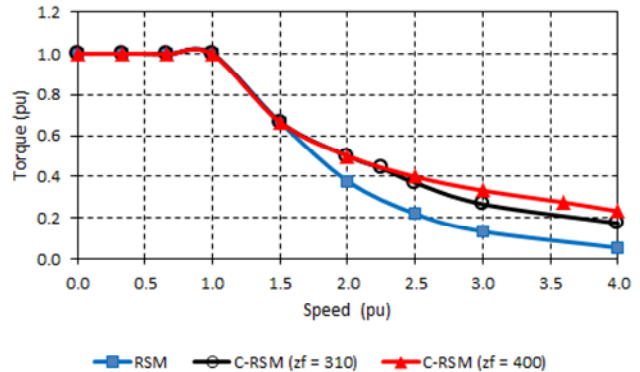


Figure 5. Torque versus speed of RSM and C-RSMs.

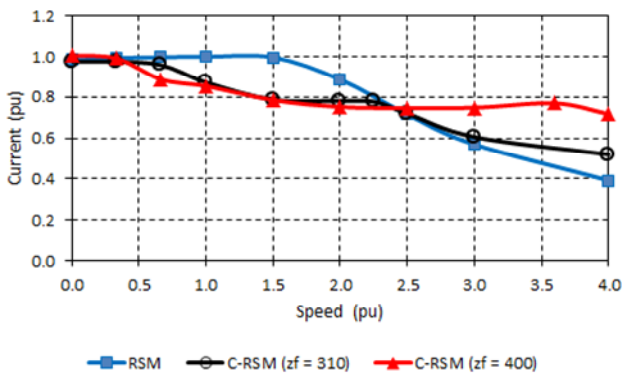


Figure 6. Stator current versus speed of RSM and C-RSMs.

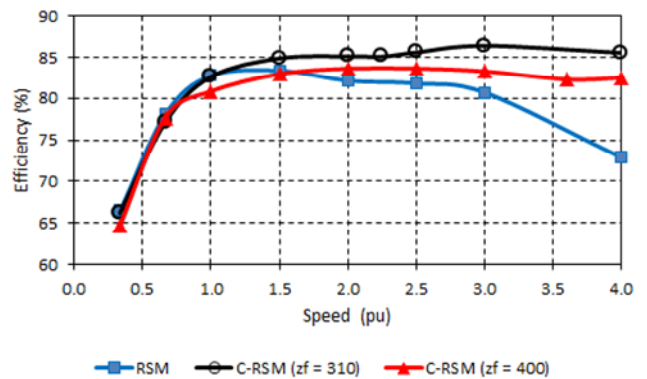


Figure 10. Efficiency versus speed of RSM and C-RSMs.

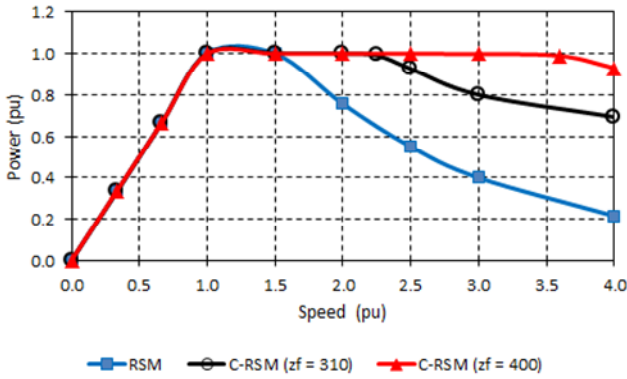


Figure 7. Shaft power versus speed of RSM and C-RSMs.

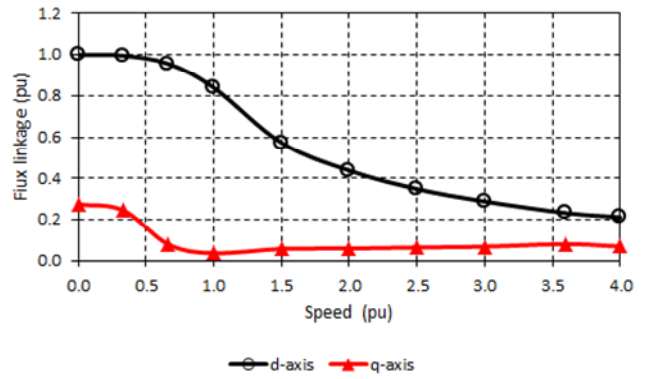


Figure 11. Stator dq flux linkages versus speed of C-RSM ($z_f=400$).

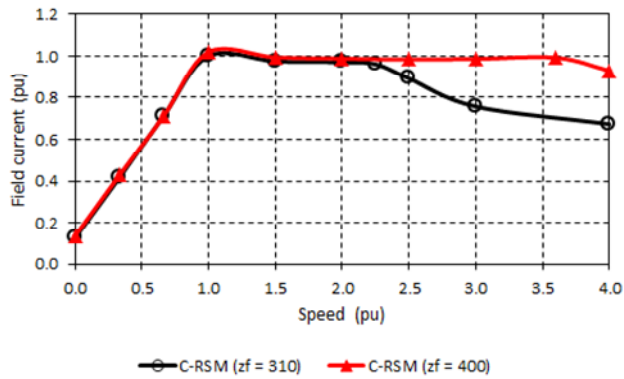


Figure 8. Field (DC-link) current versus speed of C-RSMs.

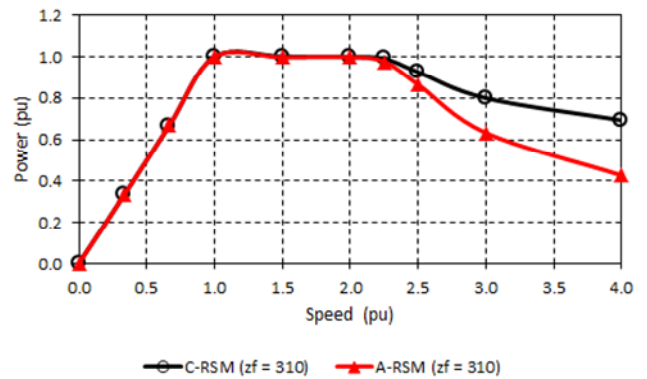


Figure 12. Shaft power versus speed of C-RSM and A-RSM.

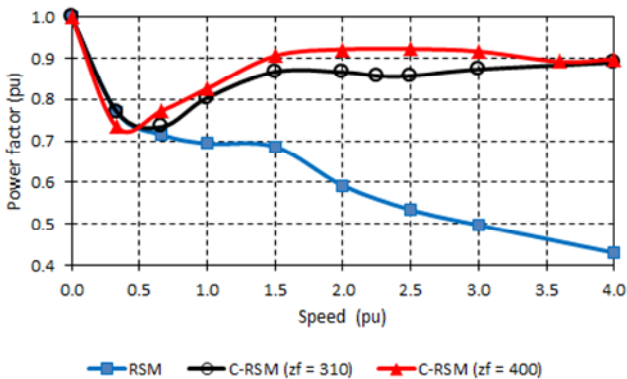


Figure 9. Power factor versus speed of RSM and C-RSMs.

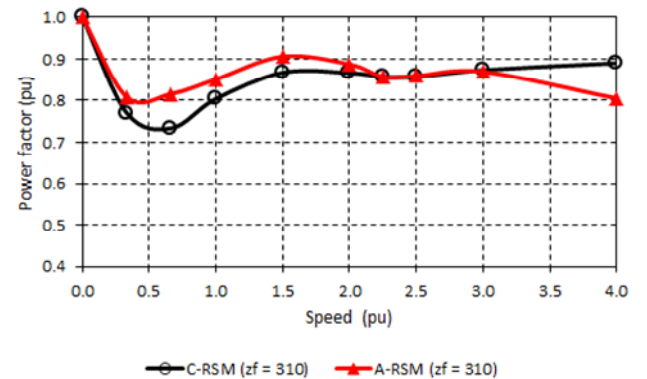


Figure 13. Power factor versus speed of C-RSM and A-RSM.

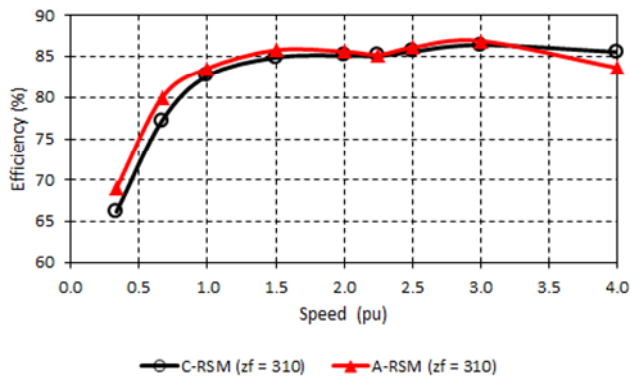


Figure 14. Efficiency versus speed of C-RSM and A-RSM.

VIII. MEASURED PERFORMANCE RESULTS

The 1.4 kW RSM with a compensated rotor winding with $z_f = 310$, has been built and tested. The wound rotor and rotor lamination are shown in Fig. 15. A photo of the experimental setup is shown in Fig. 16. In the test system two back-to-back inverters are used with the common DC-link available for connecting the compensating winding of the RSM. The one inverter powers and controls the induction machine as load and the other inverter the RSM under test. A torque transducer is connected between the two machines to measure the shaft torque.

The measured results of torque, shaft power and current versus speed for both the uncompensated and compensated drives are shown in Figs. 17 – 19. In the field weakening speed range the motor supply voltage was limited throughout at 400 V line. From these results the effect of the compensating winding on the performance of the machine in the field-weakening speed range is clear. The measured results confirm the analytical predicted performance of the drive, although only to some extent in the high speed region due to the high wind and friction losses.

The compensated RSM drive was also tested dynamically by reversing the torque signal command from rated motor torque to rated generator torque. The result of this change in shaft torque on the DC-link (field) current is shown in Fig. 20. It can be observed that the amplitude of the negative DC-link current during generating is lower than the amplitude of the positive DC-link current during motoring. This can be explained by the fact that for the same shaft power the output DC-link power is much less and so, thus, the DC-link current. Also under generator operation the DC-link bus voltage slightly increases as shown in Fig. 20, and hence the DC-link current decreases slightly further. The lower negative field current implies that compensation for a given shaft power is less during generator operation than during motor operation.

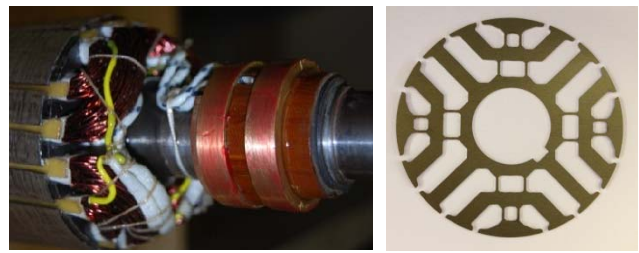


Figure 15. Wound rotor and rotor lamination of compensated RSM.

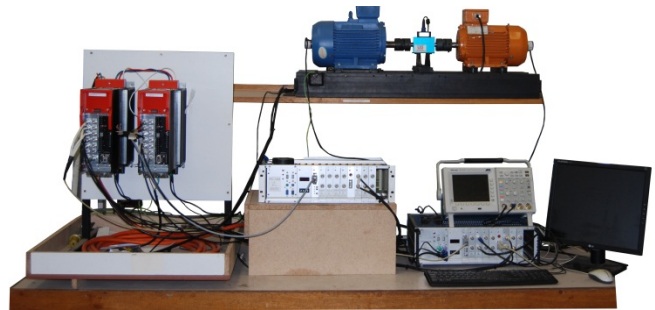


Figure 16. Test system with back-to-back inverters (left) and RSM (orange) and induction load motor (blue).

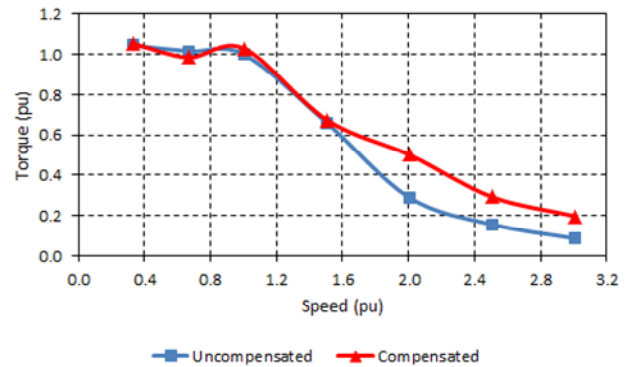


Figure 17. Measured torque versus speed of RSM and compensated RSM.

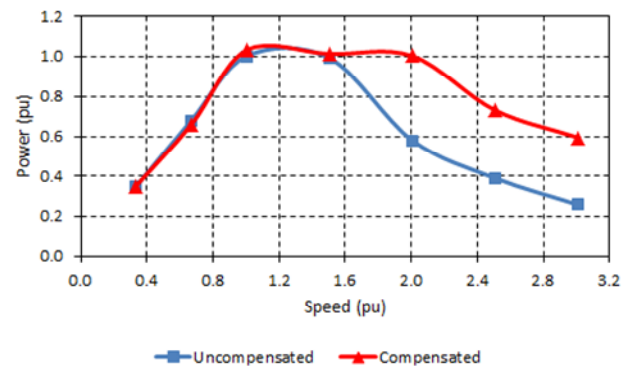


Figure 18. Measured shaft power versus speed of RSM and compensated RSM.

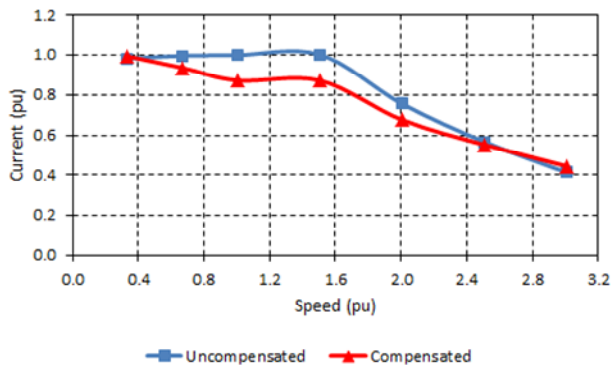


Figure 19. Measured current versus speed of RSM and compensated RSM.

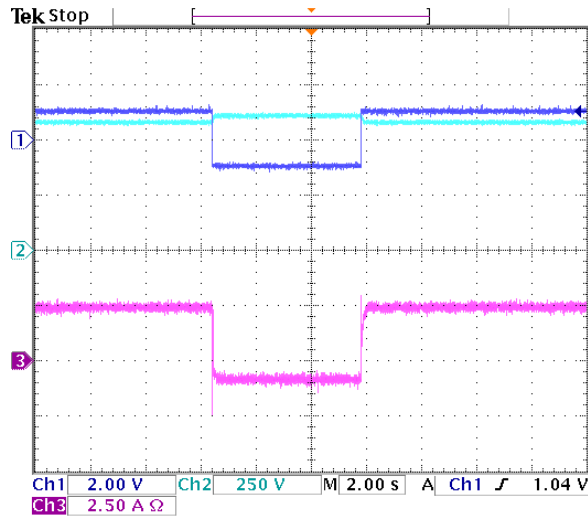


Figure 20. Measured DC-link (field) current and DC-link bus voltage of compensated RSM drive with rated-torque reversal (Ch1= torque signal, Ch2 = DC-link bus voltage, Ch3 = DC-link (field) current).

IX. CONCLUSIONS

The proposed C-RSM and A-RSM drives, using the DC-link current as feed-current through a compensated or assisted winding on the rotor, are shown to improve the power factor, efficiency and CPSR performance of the RSM drive substantially. The stator current of the C-RSM and A-RSM drives at full load is lower, which implies that the inverter operates at a higher efficiency. The efficiency and power factor of the A-RSM is found to be better than that of the C-RSM. The CPSR of the A-RSM can be extended by using a small amount of permanent magnet material on the q-axis of the rotor, as in [5].

It is clear from the results that the number of turns of the rotor winding plays an important role in the performance of the C-RSM drive. A higher number of rotor winding turns results in a wider CPSR but lower efficiency, and vice versa.

There is, thus, a design tradeoff between efficiency and CPSR that depends on the number of rotor winding turns. It is shown that the C-RSM can have a CPSR of 3.5 per unit, with 90 % power output at 4.0 per unit speed.

The important advantage of the proposed drive is that no additional power electronic converter is used. Also the inductance of the rotor winding acts as part of the DC-link filter inductance, reducing the size of the installed filter inductance. Position sensorless control may also benefit from additional voltage signal information from the rotor winding. The advantages of the drive, however, are at the expense of a large amount of copper in deep slots of the rotor, which is necessary to keep the efficiency of the machine at a required level.

APPENDIX

The constants c_1 , c_2 and c_3 of (14) are determined as follows:

$$c_1 = P_{s(i)}$$

$$c_2 = \frac{P_s(I_{s(i)}) - P_s(I_{s(ii)})}{I_{s(i)} - I_{s(ii)}} \quad (15)$$

$$c_3 = \frac{c_2}{I_{s(i)} - I_{s(iii)}} - \frac{P_s(I_{s(ii)}) - P_s(I_{s(iii)})}{(I_{s(ii)} - I_{s(iii)})(I_{s(i)} - I_{s(iii)})}$$

REFERENCES

- [1] J.J. Germishuizen, F.S. Van der Merwe, K. Van der Westhuizen, and M.J. Kamper, "Comparative study of performance of reluctance synchronous and induction machine drives for electrical multiple units", in Proc. IEEE IAS Annu. Meeting, Rome (Italy), pp 316-323, October 2000.
- [2] A. Bogliette, A. Cavagnino, M. Pastorelli, A. Vagati, "Experimental comparison of induction and synchronous reluctance motor performance", in Proc. 40th IEEE IAS Annu. Meeting, pp. 474-479, October 2005.
- [3] C. Rossi, D. Casadei, A. Pilati, and M. Marano, "Wound rotor salient pole synchronous machine drive for electric traction", IEEE IAS Annual Meeting, Tampa (USA), Oct. 2006.
- [4] I. Boldea, G.D. Andreescu, C. Rossi, and A. Pilati, "Active flux-based motion-sensorless vector control of DC-excited synchronous machine", in Proc. IEEE Energy Convers. Congr. Expo. (ECCE), San Jose, CA (USA), pp. 2496-2503, Sep 2009.
- [5] V. Coravan-Schramel, I. Boldea, G.-D. Andreescu and F. Blaabjerg, "Active-flux based motion sensorless vector control of biaxial excitation generator/motor for automobiles (BEGA)", in Proc. IEEE Energy Convers. Congr. Expo. (ECCE), San Jose, CA (USA), pp. 2131-2138, September 2009.
- [6] M.J. Kamper, F.S. van der Merwe and S. Williamson, "Direct finite element design optimisation of the cageless reluctance synchronous machine", IEEE Trans. on Energy Conversion, vol. 11, no. 3, pp. 547-553, Sep 1996.
- [7] M.J. Kamper and A.T. Mackay, "Optimum control of the reluctance synchronous machine with a cageless flux barrier rotor", SAIEE Trans., vol 86, no. 2, pp. 49-56, June 1995.